
The lineage of the line: space syntax parameters from the analysis of urban DEMs

Carlo Ratti

SENSEable City Laboratory, Massachusetts Institute of Technology, room 10-485,
77 Massachusetts Avenue, Cambridge, MA 02139, USA; e-mail: ratti@media.mit.edu

Received 10 May 2004; in revised form 8 February 2005

Abstract. A number of shortcomings of space syntax—a well-known technique of urban analysis—were recently discussed in the scientific literature. They are mostly traceable to the reliance in space syntax on the ‘axial map’: a simplified line-of-sight description of the city, which is then analysed based on its topology. This paper explores how another type of urban representations—namely the urban digital elevation model (DEM), a raster map which stores building heights—could prove helpful in providing complementary information to space syntax. Although the use of DEMs is common in the geosciences, their application in urban studies is more recent and shows promise. This paper presents several analysis algorithms to derive urban lines of sight, viewsheds, travelling time maps, and simulations based on cellular automata. The relevance of the approach is discussed, suggesting that it could effectively complement traditional space syntax in the coming years.

1 Introduction

How shall we quantify the influence of the urban configuration on the use of streets and public spaces by pedestrians? This is one of the fascinating questions posed, and partially answered, by space syntax, a technique developed over the past few decades at University College London, and well known to the readers of *Environment and Planning B* (for an overview see Hillier, 1996).

With the number of practical applications growing beyond pedestrian movement [from air pollution modelling to occurrence of burglaries (<http://www.spacesyntax.com>)] space syntax has recently come under scrutiny (see Batty, 2004; Hillier and Penn, 2004; Ratti, 2004a; 2004b; Steadman, 2004). Shortcomings seem mostly to be traceable to its reliance on the ‘axial map’, a simple longest-line-of-sight mapping derived from a city’s planimetric representation and analysed on the basis of its topology.

Although a simplified format and a concise representation of street networks would probably have been a necessity in the early days of space syntax, when computing resources were scarce, it is possible today that a more complete analysis based on a richer support would be helpful to understand the ‘social logic of space’. The success of the use of the axial map “is not to say that a more refined form of analysis... would not yield even better results” (Hillier et al, 1993, page 35). New algorithms could probably be written to analyse the full complexity of urban texture and take into account its metric properties.

What would then be the best support to describe the city? A full three-dimensional (3D) manipulation of large urban areas is computationally very costly. Even simple algorithms for shadow casting, which are now included in most software packages such as AutoCAD (Autodesk, <http://www.autodesk.com>), do not pose problems at the scale of individual or groups of buildings but fail on larger urban areas because of excessive vectorial complexity. This paper aims to test the possibility of using a very simple raster model of the urban geometry: the so-called digital elevation model (DEM), which is shown in figure 1 and figure 2 (see over). The DEM is a compact way of storing urban 3D information using a 2D matrix of elevation values; each pixel represents building height and can be displayed in shades of grey as a digital image.

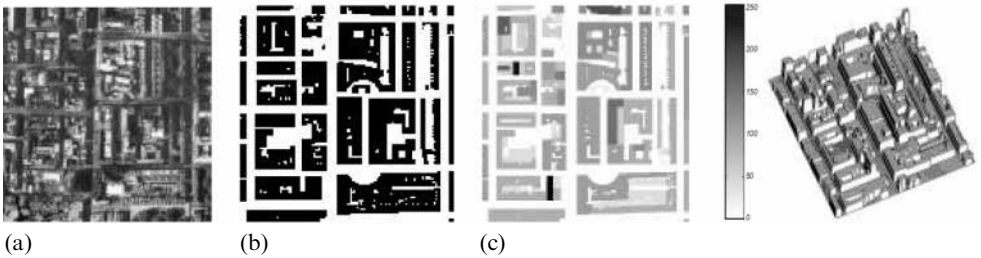


Figure 1. Case-study site in central London in an aerial image (a), in a black and white ground map showing built and unbuilt areas (b) and in the digital elevation model format (c).

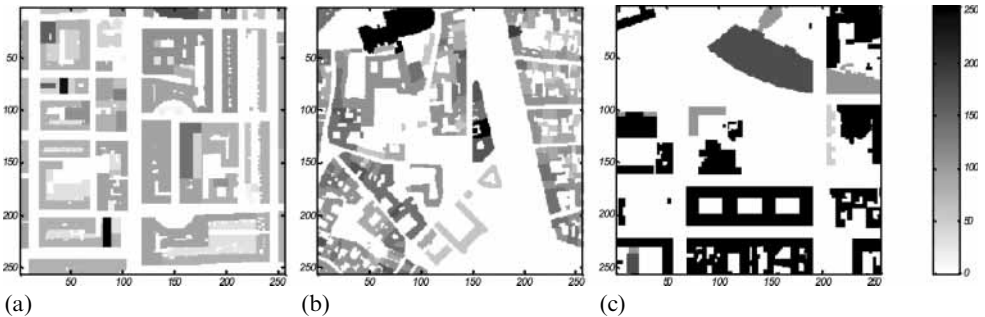


Figure 2. Case-study sites in (a) central London, (b) Toulouse, and (c) Berlin represented in digital elevation model formats.

The DEM format was initially introduced and defined in the geosciences, but it is becoming increasingly common in urban areas thanks to the development of fast 3D surveying techniques such as lidar.

The analysis of DEMs with image-processing techniques has already proven to be an effective way of storing and handling urban 3D information, conducive to a number of urban analyses (Ratti and Richens, 2004). Could it be used to derive some measures of urban configuration that could complement traditional space syntax? A number of algorithms to analyse urban DEMs are described below. They have been developed using the Matlab software (<http://www.mathworks.com>), a well-known package for doing numerical computations with matrices and vectors. Matlab's extensive matrix capabilities are supplemented by different toolboxes, among which is the 'image processing toolbox', with elaborate graphics outputs.

2 Visibility analysis: lines of sight

The basis of most space syntax techniques is the tracing of lines of sight. Initially, this was an instrumental procedure in the creation of axial maps. Later, it became a way of studying urban configuration per se. In this sense, important references are the work of Peponis et al (1998), who analyse the visible relations between the surfaces that bound and subdivide space, and Batty (2001a), who describes the extent of lines of sight in the urban context from variable vantage points. Batty and Ranna (2004), Rana (2003), and Turner (2003) should also be mentioned.

In fact, visibility parameters are considered fundamental in many disciplines that deal with the interaction between man and his or her environment: from perception psychology (see, for example, Gibson, 1966) to human and urban ethology (for a review of articles on human ethology and on an evolution approach to the perception of urban spaces see Atzwanger and Schäfer, 1999).

The simplest possible parameter to characterise visual fields is the length of the line of sight. In other words, this is how far the eye can see in a given direction. How can this parameter be calculated in the street network from a DEM? Note first that when the urban ground is flat this problem is simply 2D and that 3D information from the DEM is not required: a binary black and white image of the street networks will suffice (let us assume that streets are given the value 1 and buildings the value 0).

A fast Matlab algorithm can then be written based on the iterative shifting of this image (similar to that presented by Ratti and Richens, 2004). Let us start by defining the two components of the vector pointing in the chosen direction v . Then the components of an opposite vector in the direction $v + 180^\circ$ are computed and scaled so that the larger of the x and y components is just 1 pixel. If the image is translated by the x and y components and intersected with the original image, so as to preserve only pixels corresponding to streets (so that 'black is the sum of blacks'), a progressive erosion of the street network in the direction $v + 180^\circ$ is obtained. This erosion, when repeated and coupled with the addition of each subsequent image to the previous one, results in the value of the length of the lines of sight.

Incidentally, it is noted that this technique for computing the length of the line of sight in a given direction is very similar to the one developed by Batty (2001b), although he implemented it using cellular automata. Batty's algorithm is based on filling the street network with agents programmed to move in a given direction. Then the count of how many steps the agents have walked before bumping into a façade (an operation similar to repeated shifting) gives the length of the lines of sight.

A number of images showing the length of lines of sight in London at different azimuths are shown in figure 3. From results such as these, computed at regular intervals (say each 10° , or 36 directions), a number of different aggregates can be calculated: average length of the lines of sight (figure 4); maximum length of the lines of sight (figure 5, see over); maximum of the sum of the length of the lines of sight in two opposite directions (figure 6, over); minimum length of the lines of sight (figure 7, figure 8, over).

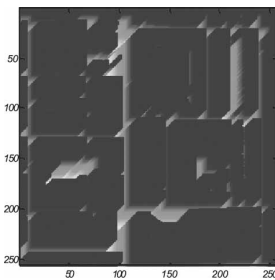


Figure 3. Length of the lines of sight at 45° direction. Colour versions of figures 3–11, 13–24, and 26 can be viewed on the *Environment and Planning* website at <http://www.envplan.com/misc/b31045>.

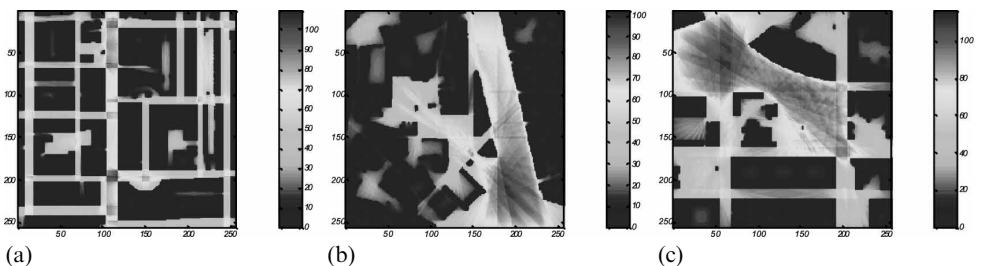


Figure 4. Average length of the lines of sight on the (a) London, (b) Toulouse, and (c) Berlin digital elevation models (32 different directions computed).

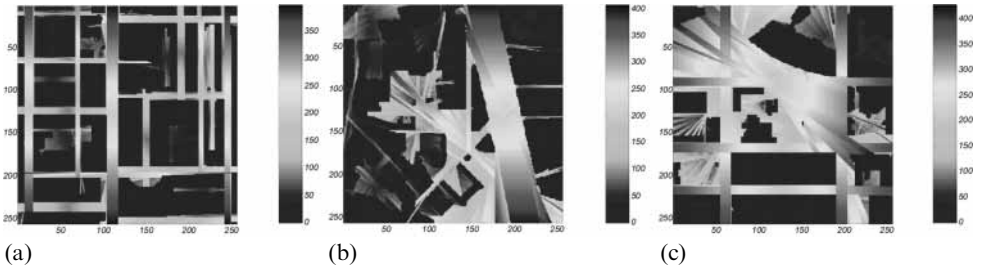


Figure 5. Maximum length of the lines of sight on the (a) London, (b) Toulouse, and (c) Berlin digital elevation models (32 different directions computed).

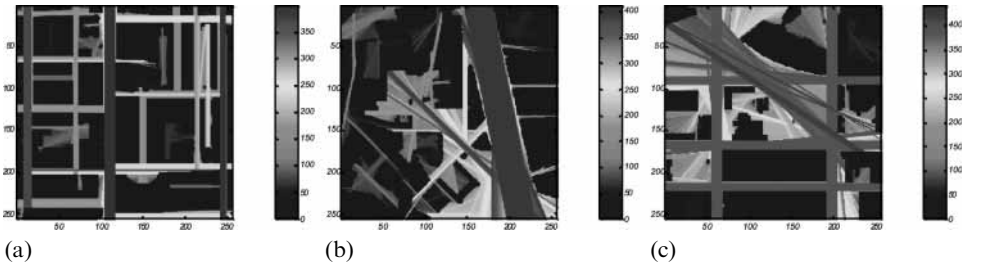


Figure 6. Maximum of the sum of the length of the lines of sight in two opposite directions on the (a) London, (b) Toulouse, and (c) Berlin digital elevation models (32 different directions computed).

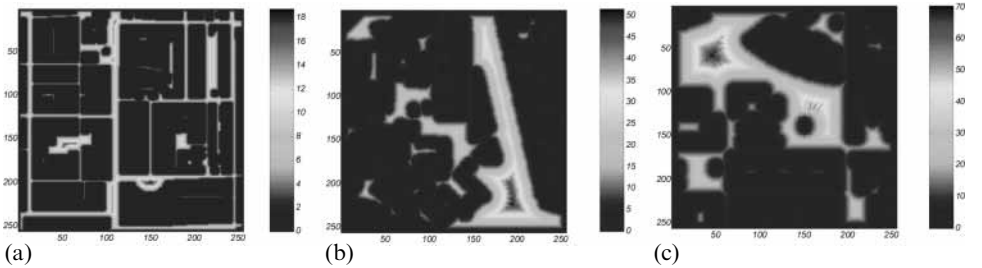


Figure 7. Minimum length of the lines of sight on the (a) London, (b) Toulouse, and (c) Berlin digital elevation models (32 different directions computed).

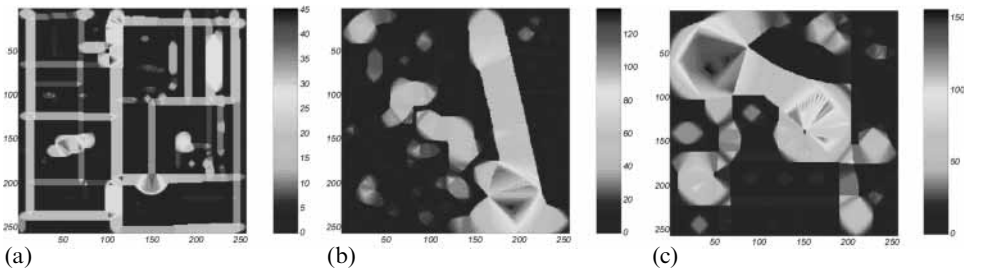


Figure 8. Minimum length of the lines of sight on the (a) London, (b) Toulouse, and (c) Berlin digital elevation models (32 different directions computed) obtained by adding values in two opposite directions.

Take the following problem: what would be the optimum location in which to open a shop, based on the simple law of maximising the urban areas from which it can be seen? Because of reciprocity this problem is equivalent to maximising the average view from the retail location: the urban areas with the greatest potential can therefore be detected on the image showing the average length of the lines of sight by thresholding all pixels above a certain value (figure 4). As can be seen, these pixels are concentrated on the edge of wide urban spaces and on block corners, where views go down two or more streets. This simple fact was probably known to traditional retailers, as documented by the custom of opening public houses and other commercial activities on corner locations.⁽¹⁾ Other applications could be thought of in advertising, by detecting the most visible urban positions.

The average length of the lines of sight for a given built density might also represent a measure of the structuring of urban space. Given a number of buildings scattered on a plane, the average length of the lines of sight would be proportional to how regularly they are arranged. In purely random conditions this value is inversely proportional to the size and density of buildings (see the appendix). Setting values obtained in real urban textures against those that would be obtained in purely random conditions, might constitute an interesting indicator of urban regularity and alignment.

The average length of lines of sight, when applied not to the street network but to city blocks and inside buildings, can also give an estimate of urban grain size. For instance, let us repeat the visibility analysis on an input image reversed, that is, with urban blocks in white and streets in black. The results, shown in figure 9, represent for each pixel the average distance from the built boundaries—or in other words, the average length of segments intercepted on the image by random lines laid down on it.

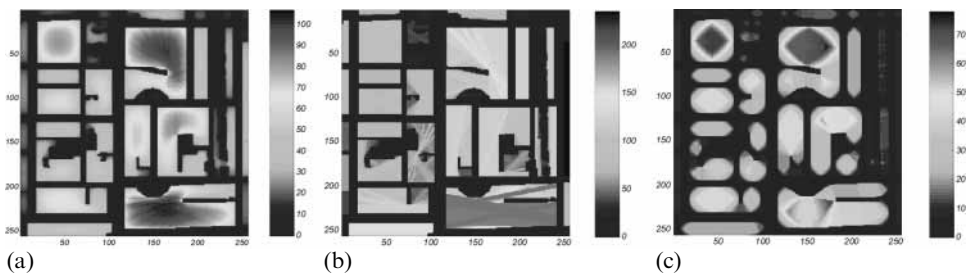


Figure 9. Average (a), maximum (b), and minimum (c) lines of sight inside building blocks on the London digital elevation model (32 different directions computed).

The minimum length of the line of sight on each pixel can be interpreted simply as the distance from two opposite façades—which in regular urban canyons is just the width of streets (in open areas or places of more complex geometry this is not the case).

A number of other applications for the above parameters are summarised by Batty (2001a), who shows how some of them can be used to study the town centre of Wolverhampton. However, the calculation of lines of sight in the street network remains fundamentally a 2D operation. The question of whether visibility analysis can be extended to three dimensions, making full use of DEM capabilities, is discussed below.

⁽¹⁾ Visibility information could be combined with the results of environmental analyses, providing a richer estimate of locational potential. For instance, in the case of a public house with outdoor seating the aim might be to maximise illumination and view of the sky as well as ground visibility. Also, if maximum group visibility is very beneficial for, say, a McDonald's fast-food outlet, it can be less important or even detrimental in other cases—such as that of an exclusive restaurant which tries to restrict its clientele just to a few habitués.

3 Height to width

It has been stated above that the minimum length of the line of sight on each pixel can be interpreted simply as the distance from two opposite façades. The simplest way to add 3D information to this measure is to analyse the *height-to-width ratio* (also called H/W or *aspect ratio*).

The H/W ratio has a long history in disciplines such as urban climatology (Oke, 1988); there it has been used to describe flow conditions at the street scale and to highlight urban areas with poor ventilation and pollution dispersal (high height-to-width) or little shelter (low height-to-width). In our context it can provide an interesting measure of urban enclosure.

The first issue to tackle is its definition. This is trivial when dealing with canyons of uniform height, such as those commonly found in the literature, but becomes trickier in real cities, which often present irregular building patterns. In some cases, even the notion of ‘canyon’ blurs. In squares, for instance, a number of height-to-width values can be imagined, according to the selected orientation. Problems also arise in the case of street junctions or loose sprawling urban textures.

As a general case, it can be considered that height-to-width is a function of orientation. The definition that has been adopted for each direction α is based on assigning to each pixel a value of height-to-width based on the two obstruction angles in the directions α and $\alpha + 180$. Expressed as a formula:

$$(H/W)_{P_i} = \frac{h_{i,1} + h_{i,2}}{2(w_{i,1} + w_{i,2})}$$

Notations refer to figure 10, where $(H/W)_{P_i}$ represents the value of the height-to-width ratio at point P_i , h_i represents the height of the obstructing buildings in two opposite directions, and w_i the horizontal distance of those buildings from point P_i .

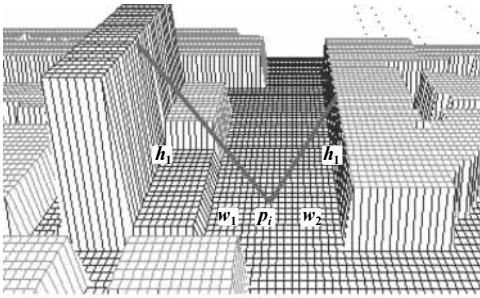


Figure 10. A possible way to calculate aspect ratios on digital elevation models, based on the obstruction angles in opposite directions: $(H/W)_{P_i} = (h_{i,1} + h_{i,2})/2(w_{i,1} + w_{i,2})$.

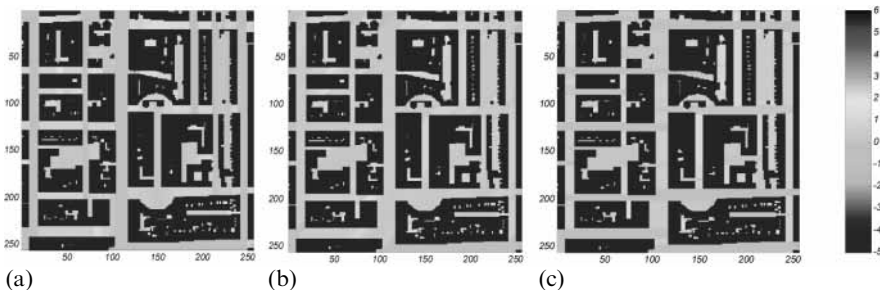


Figure 11. Height-to-width ratios in different directions in central London, scanned at (a) 0° , (b) 45° , and (c) 90° .

A modification of the algorithm presented in Ratti and Richens (2004) allows the calculation of the obstruction angle in different directions, from which height-to-width values can be derived (figure 11).

4 Visibility analysis: the viewshed or isovist

The simplest approach to characterise visibility in three dimensions is to detect all areas on the DEM that can be seen from a given vantage point (as opposed to those that are invisible). This is a well-known operation in the geosciences, and often appears as a built-in function in GIS packages. It is usually referred to as *viewshed* calculation, although the architecture and urban study community prefers the term *isovist* analysis (see, for example, Benedikt, 1979).

The viewshed has a number of important applications: from the topical assessment of the best location to place microwave transceivers for telephone, FM, radio, and television (or other appliances which require line-of-sight communication), to forest fire observation, visual impact planning, or detection of hidden zones for military purposes. It is also a relevant measure in architecture and urban studies, as explained by Benedikt (1979), who grounds its analysis in perception psychology. It is clear that the viewshed from a given point describes how extended the sources of visual information from that point are; and that therefore it should play some role in human behaviour. To date, however, with a few exceptions such as Campos (1997), “The direct empirical testing of how some human behaviours and perceptions might correlate with isovists, isovists measures, and isovists fields, however, remains to be done” (Benedikt, 1979, page 59). In the future, great help in the validation of the role of the viewshed or viewshed-related measures as determinants for urban movement might come from the great collection of observational data that have been gathered by the Space Syntax Laboratory in London during the past decades.

Algorithms to compute the viewshed are computationally intensive and time consuming. A vast number of them have been suggested in recent years (see, for instance, Nagy, 1994) and big efforts have been and are still being made to speed them up and improve their performance (for instance, Franklin and Ray, 1994; Van Kreveld, 1996; Wang et al, 1996).

The algorithm that has been developed here is rather fast and gives good results on fragmented and discontinuous DEMs, such as urban ones (unlike some algorithms developed in the geosciences, which work mostly with smooth topographical surfaces). It is based on the adaptation of the shadow-casting routine (see Ratti and Richens, 2004) and does not appear to have been used before. This routine casts shadows on a DEM, based on the computation of the shadowing volume. The latter was obtained with iterative shifting of the DEM and its simultaneous reduction in height. It represented the height of the separation surface between shadow and light under a beam of parallel rays.

The viewshed algorithm works fundamentally in the same way, although light rays are now not parallel but divergent. It is like having a light bulb at a certain position in the city and projecting rays all around [the light bulb analogy is used by Benedikt (1979) and O’Rourke (1987)]. The viewshed is simply the collection of all illuminated areas.

How can we simulate divergent light rays on a DEM? If parallel rays require iterative shifting, divergent rays can be simulated by recursively applying a polar deformation to the image. This is a simple operation in Matlab and can be implemented by transforming the matrix coordinates of the DEM into polar coordinates centred at the vantage point (radius r and angle θ), applying a radius increase dr , and going back to image coordinates. The process is presented in figure 12 (see over) for different dr .

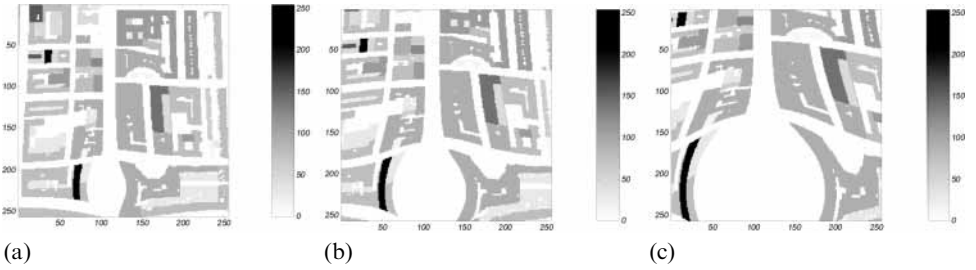


Figure 12. Polar deformation of the London digital elevation model from point (220, 110) in image coordinates; deformation of (a) 14, (b) 35, and (c) 70 pixels.

This ‘polar deformation’ subroutine allows the structure of Ratti and Richens’ shadow-casting algorithm to remain unchanged. The equivalent of the shadowing volume described in section 2.5 is presented in figures 13–15 (both in grayscale and colourmap, for the sake of visual clarity). As in the shadowing algorithm, the detection of the points where the height of the shadowing volume is higher than the height of the DEM allows the identification of shadows (black). All other points (white) are those illuminated by the imaginary light bulb: they constitute the viewshed from the given vantage point.

When addressing pedestrian movement, the viewshed should be calculated from a person’s eye height. Because all buildings are higher than that level, however, the same results would be obtained by calculating the viewshed from a vantage point on the ground. In this case the algorithm described above can be used, or alternatively a slightly modified and faster version. The latter avoids the calculation of the shadowing volume and simply relies on the polar deformation of the image and its repeated intersection with its predeformed condition. This process progressively ‘kills’ all rays obstructed by buildings. Distance from the vantage point can also be encoded on this 2D image, as shown in the colour viewshed presented in figure 16.

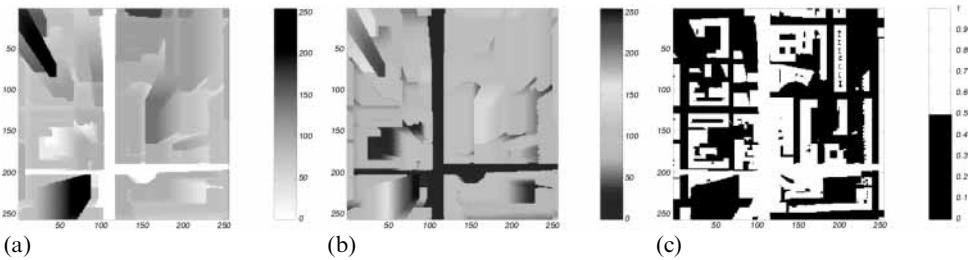


Figure 13. Central London: shadow volume in grayscale (a) and colourmap (b) produced by an imaginary light bulb placed at the point (192, 113) in image coordinates, height 187m, and (c) shadowed (black) and illuminated (white) pixels, which constitute the viewshed.

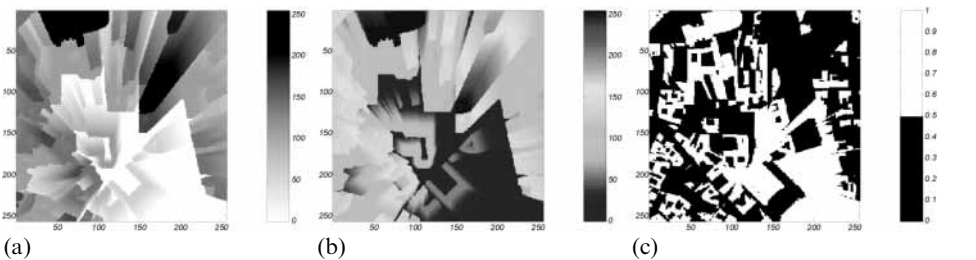


Figure 14. Central Toulouse: shadow volume in grayscale (a) and colourmap (b) produced by an imaginary light bulb placed at the point (192, 113) in image coordinates, height 187 m, and (c) shadowed (black) and illuminated (white) pixels, which constitute the viewshed.

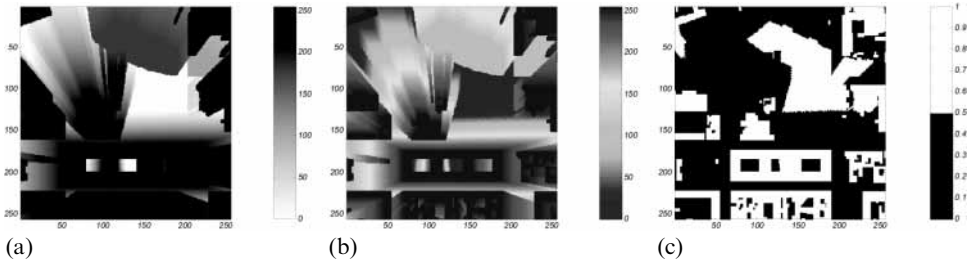


Figure 15. Central Berlin: shadow volume in grayscale (a) and colourmap (b) produced by an imaginary light bulb placed at the point (192, 113) in image coordinates, height 187 m, and (c) shadowed (black) and illuminated (white) pixels, which constitute the viewshed.

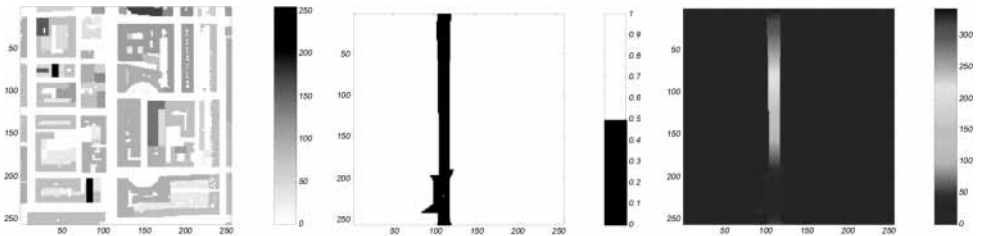


Figure 16. Viewshed (or view polygon) from the point (220, 110) in image coordinates.

The viewshed at ground level is always a connected polygon.⁽²⁾ Conversely, in three dimensions, disconnected regions appear, as can be seen in figures 13–15. In that case a distinction is made between the area connected to the vantage point, which is called by some authors the ‘near viewshed’, and the scattered areas around.

5 Metric distance and integration

In addition to the concept of viewshed, the quest of space syntax to model pedestrian movement in urban areas could benefit from other analyses developed in the field of raster GIS, such as algorithms for calculating the accumulated distance from a given origin (say, point A). On a flat surface, for instance, the accumulated distance is a cone centred in A, which contains on each pixel the Euclidean distance between that point and A (figure 17). On a DEM representing a mountainous area, it is a more complex function, representing the distance from A following the actual topography, that is, moving up and down the slope on geodesic paths.

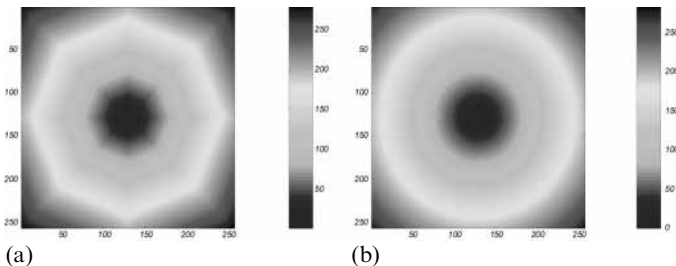


Figure 17. Accumulated distance on a flat surface, with octagonal approximation (a) and precise Euclidean distance (b).

⁽²⁾This fact can be proven by contradiction (*reductio ad absurdum*) in the following way. Assume that there is a point A belonging to the viewshed and not connected to the vantage point V. That would imply that the line of sight, which passes on the ground, is broken. Therefore point A cannot belong to the viewshed.

The idea of accumulated distance can be generalised beyond the Euclidean distance, to include aspects such as the cost of moving through each pixel, and the pleasure of enjoying landscape views. In this section the use of the accumulated Euclidean distance in urban areas (when movement is constrained to the street network) is presented—a simple investigation whose potential does not yet seem to have been fully explored in urban analysis.

Algorithms for calculating accumulated distances on surfaces are structured backwards, that is, from an origin A outwards. They are called spreading algorithms [see, for example, Douglas (1994) or, more generally, in the context of computer programming, Cormen et al (1990)] and are based on the following procedure:

- (1) Start with the origin or source pixel A and assign to it the value 0.
- (2) Take its eight neighbouring pixels (the pixel neighbourhood), and assign to each of them the value of the source (0) plus their distance from it (the pixel distance d to the four lateral neighbours, and $d2^{1/2}$ to the corner neighbours).
- (3) Repeat the operation, whereby at each time pixels on the boundary of those that have already been assigned a value are assigned the lowest value from their neighbourhood plus the travelling distance from the neighbourhood to them; this links each cell to the one which is in the least costly direction to a source cell (back-linking).
- (4) Stop when all pixels are set.

In other words, a path made up of increments is built (figure 18). The operation is analogous to that of a non-mass-conserving fluid spreading with uniform velocity in the street network from the source point A (a more rigorous analogy is that of spreading waves, which is used, for instance, by Tomlin, 1990).

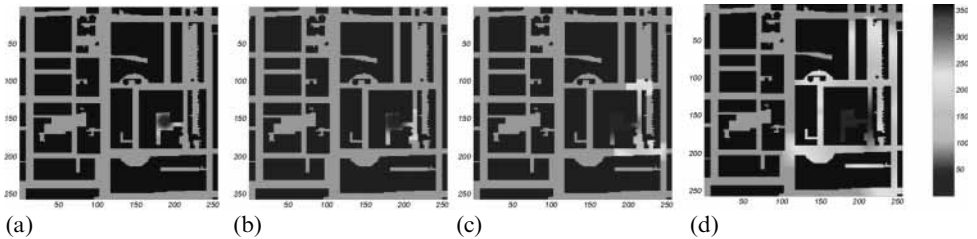


Figure 18. Accumulated distance in the central London street network from point (152, 188) in image coordinates after (a) 20, (b) 40, (c) 80, and (d) 160 iterations; note the similarity with a spreading fluid.

Because of the discontinuous nature of pixel operations, this process causes some approximation: on a flat plane, for instance, the above algorithm would produce octagonal patterns instead of circular ones (figure 17). However, this problem can be overcome by using corrections, such as those proposed by Douglas (1994).

Accumulated distance in central London, calculated from different points of departure, is presented in figure 19. It is interesting to plot these results in axonometric form: in fact, it can be proved that slope lines (that is, gradient lines) on the axonometric surface trace the shortest path from any pixel to point A.⁽³⁾ Therefore, a small ball without inertia rolling down the surface will find its shortest route to the origin. In the case of a flat plane, whose conical accumulated distance surface is plotted in figure 20, shortest paths are given by divergent straight lines from the origin: this proves that on the plane the shortest path between two points is a straight line, as everybody knows.

⁽³⁾The computation of least-cost path is a long-standing research problem. Well before the proliferation of computer technology, manual methods existed to optimise the path between two points, such as Lindgren (1969) and Warntz (1957).

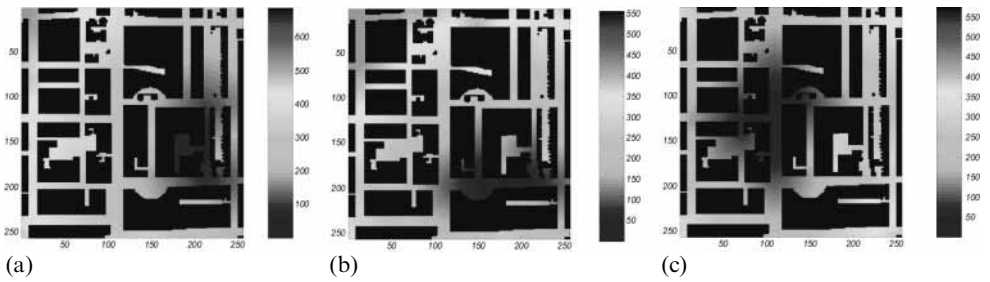


Figure 19. Accumulated distance in the central London street network from different starting points.

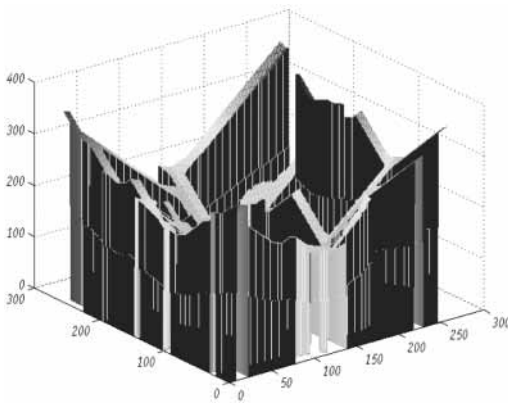


Figure 20. Three-dimensional graph of figure 19 representing accumulated distance in central London; an interesting property of this surface is that a ball without inertia falling on it would find its shortest path to the origin.

The same concept of Hillier's integration can be implemented with Euclidean distance instead of topological distance (number of turns in the lines of sight). Integration at a certain point in space could be obtained by taking the average length of the journeys to go to all other points. The process could then be repeated for different origins, showing the changes in the accessibility of the street network from each origin and providing an indication of the deformation of space because of the blocking effect of buildings.⁽⁴⁾

However, the most exciting thing about accumulated distance is that it can be generalised beyond Euclidean measures, as explained below.

6 Generalised distance

In the description of spreading algorithms above, the notion that proximity is somehow related to motion was tacitly introduced. In fact, the maps that represent accumulated Euclidean distance can also be interpreted in terms of travelling time or other accumulating quantities. As stated by Tomlin (1990), when discussing the calculation of accumulated cost surfaces in GIS:

“As a snail makes its way across a garden, as an echo makes its way across a canyon, or as an airplane makes its way across a continent, physical distance accumulates, be it in inches, meters or miles. But so do minutes. And so can dollars, or gallons of fuel, or even levels of environmental impact. For many applications, these units of ‘distance’ will in fact yield measures of relative position that are much more meaningful than conventional measures of physical separation.”

⁽⁴⁾ In fact, the accumulated distance algorithm can be interpreted in terms of graphs, in which each pixel is a node; it is therefore very similar to space syntax analysis.



Figure 21. Isochronic passage chart for travellers, showing “the shortest number of days journey from London by the quickest through routes and using such further conveyances as are available without unreasonable cost.” Note that the gradient of colour is proportional to travelling speed; this means that travel by sea is generally faster than travel overland, although the latter changes from one location to the other (the more developed road and railway networks in Europe allow faster travelling, than, say, in central Africa or Asia). From Galton (1881).

The maps in figure 19, for instance, can be interpreted as isochronic maps (isochrones are lines of equal temporal distance from some specified central point).

The use of time mapping as a surrogate of distance is quite common. Maps of the universe define the relative position of stars and planets in terms of light-years, which represent the distance travelled by light in a vacuum during one year. Closer to us, figure 21 shows a 19th-century world map where isochrones of different colour separate areas which may be reached in a certain number of days “by the quickest through routes and using such further conveyances as are available without unreasonable cost” (Galton, 1881). It is interesting to note that travel by sea was generally faster than by land, as shown by the lower gradient between temporal zones. Furthermore, fast transport systems locally affect the gradient, as does the railroad through the Rocky Mountains in the western USA (it is faster to reach San Francisco than closer places north or south of Salt Lake City).

Isochrones are a simple way to superimpose time data on topographical maps. Alternatives, however, are available, as *cronogeographic representations* [see Vasiliev (1997) for a comprehensive review of time representation on maps]. Unlike isochrones, which preserve the geometry of a map and simply add time information, cronogeographic representations require the distortion and remapping of space. A well-known example is the distorted and shrunk map of Europe, which shows the travelling effects of introducing high-speed trains across the continent. In cronogeographic representations space is less recognisable, but information is graphically more exciting and, eventually, more conducive to urban analysis. In general, they can help detect physical barriers and diffusion patterns.

For instance, in figure 22 a portion of the London case-study site has been distorted based on travelling time: radial distance from the centre of the image (departure point) is proportional to travelling time, which means that concentric circles are

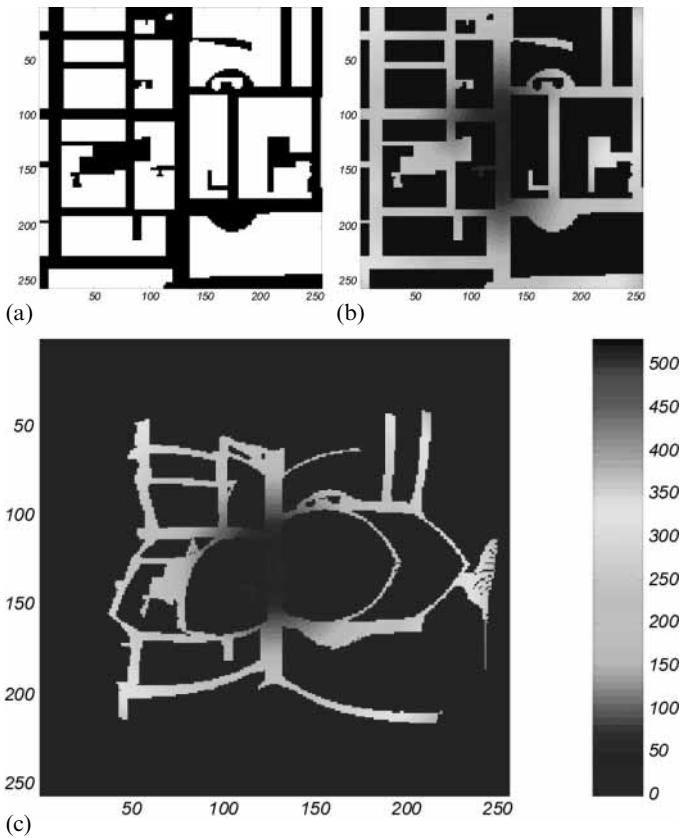


Figure 22. Chronogeographic transformation of a portion of the central London case study: street network (a), isochrones from the centre point (128, 128) in image coordinates (b), and deformation of the map (c) so that radial distance from the centre point is proportional to travelling time (concentric circles are reached simultaneously).

reached simultaneously. As an example, a fire originating in the centre of the image and spreading uniformly in the street network, would propagate in a circular way. Note that the big courtyard on the right-hand side of the image has undergone a centrifugal mirror shift, thanks to its low accessibility from the departure point. Its topological connections, however, remained unchanged. All points in the original map have their correspondent point in the deformed one, although sometimes two points can be merged into a single one (the transformation is not reversible).

The above transformation, however, is very specific to a given starting point, from which all journeys originate. In a more general way, it is possible to compute travelling time from all origins to all destinations, and to remap space fully according to it. This operation does not preserve topology and has not been implemented here because of its computational tediousness.

Another way to generalise accumulated distance maps, beyond travelling time, is to introduce a cost-of-passage function, also called friction or impedance, which can be stored on a new image other than the DEM. This function represents the cost of crossing each pixel, not just in terms of time or Euclidean distance, and is best explained with an example. Imagine that the effort needed to walk from a given origin to any other point on a mountainous DEM is to be determined. Imagine also that the criterion of effort is based solely on terrain slope: the steeper the area crossed, the greater the effort.

It is then possible to associate with each pixel of the DEM a cost of passage function (it tells us how expensive it is to cross it) and determine, with the same spreading algorithm described above, the accumulated cost of moving from an origin to any destination.

Different factors can be collapsed onto a single cost surface: parameters such as the terrain slope, the difficulty of construction of a road, the speed of moving through the landscape or the presence or absence of a scenic view are commonly used in the geosciences. In the urban context it would be possible, for instance, to use traffic information, whereby routes jammed by cars are assigned a high cost of passage.

A generalised ‘shortest path’ can also be calculated: this is generally called the parsimonious path and minimises the cost between two points, based on the chosen criteria. Visibility information, from the viewshed analysis, can be collapsed onto the cost-of-passage surface, allowing the identification of scenic or smuggler’s paths (see, for instance, Lee and Stucky, 1998). The latter are the most hidden itineraries on the landscape and have important applications in the military context.

This sort of analysis is supported by some GIS packages, although its extension to the study of human settlements has been limited until the present. A notable exception in archaeology is the work of Llobera (2000), who calculates accumulated cost surfaces and other measures from topographical DEMs, subsequently inferring information on the potential for ancient settlements at different locations.

In architecture and urban studies these kinds of measures are not commonly used. Hillier (1996) envisages a number of them in the chapter “Future urban models: intelligent analogues of cities”, although he seems to see them mainly as prospective developments. The analysis of urban DEMs makes their calculation realistic.

7 Accessibility of buildings: the bus stop problem

So far, the accessibility of the street network has been measured. In general, however, the focus would be on the accessibility of buildings. A simple problem is the following: given a bus stop and a certain area of influence (say 5 minutes walk or 300 m), how many people could be served?

The standard answer to this problem is that of tracing circles with different radii around the bus stop and applying some standard population density. This approach, however, could give very poor results when urban areas are irregular in terms of street network and building height; tall buildings or low-rise developments would be given the same density.

A better answer can be found by using all the information stored in DEMs and calculating the catchment area of each bus stop in terms of m^2 or m^3 of buildings—then to be converted into the number of people using some occupation coefficient. The 3D information becomes therefore a measure of capacity. So far, travelling time in the street network can be calculated and all areas within a certain distance from the bus stop detected; the only thing missing is the association of buildings with streets.

A reasonable approach to associating buildings with streets seems to be to put into correspondence each pixel representing a building with its closest street pixel, using the distance from façade transformation. This has been done for the case study in central London, shown in figures 23 and 24. Increasing distances from the bus stop are considered, and its respective served areas identified (figure 25 and table 1, see over). Note the difference that would be obtained with the crude approximation of a circle centred at the bus stop, in particular in near-orthogonal urban systems in which catchment areas tend to assume a rhombic shape. Another significant difference is caused by taking building height into account.

The above process can of course be refined. First, the catchment area of the bus stop could be weighted with a probabilistic decay function, telling us the percentage

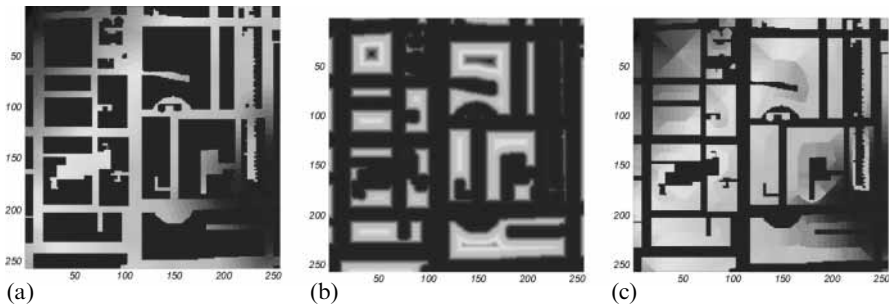


Figure 23. Accumulated distance from point (184, 244) in image coordinates (a); values are then spread inside the buildings by assigning to each pixel the value of its closest façade (c), which is determined using the Euclidean distance transform (b).

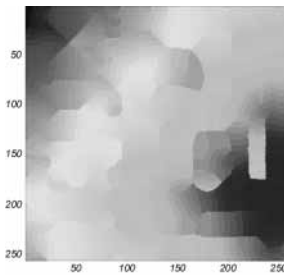


Figure 24. Combination of the images of figure 23: accumulated distance from (184, 244) in image coordinates, both in the street network and inside the buildings.

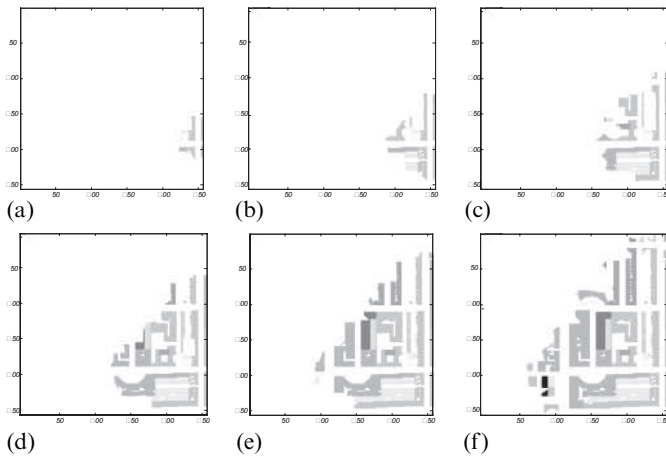


Figure 25. Portions of central London within (a) 50, (b) 100, (c) 150, (d) 200, (e) 250, (f) 300 m from point (284, 244) in image coordinates.

of built volume to take into account at different distances (this percentage would fall to zero after a certain limit, where the bus stop would no longer exert any influence). Second, if information was available on the actual position of doors and on the internal partition of buildings, accessibility could be simulated more accurately. It would be possible to run an accumulated distance where the cost of passage on façade pixels would be infinite (impermeability to movement), except for doors. This would mimic precisely the pedestrian entrance into the buildings. Also, the distance from the ground floor could be taken into account.

Table 1. Portions of central London (in m³) within various distances from point (284, 244) in image coordinates.

Distance (m)	London (m ³)
50	23 621
100	74 338
150	155 633
200	287 901
250	440 232
300	610 155

The slight increase in precision might not justify in this case the complication in the algorithm. However, other applications could be of interest. The attribution of different costs of passage to street pixels might be a way to simulate lanes at different speeds, which may be used to mimic different transport systems. Consider, for instance, underground lines and stations: the former can be represented as lanes with a low cost of passage (high speed) and an infinite cost of passage on the boundary (impermeability to adjacent areas); the latter would be breaks or entrances in the strip with infinite cost of passage, allowing access to the underground system. Extending this idea to several transport systems would allow the accumulated cost algorithm to mimic not only pedestrian but all kinds of movement in the city—therefore transforming the calculation of shortest path into an effective journey-planner optimiser.

8 Pedestrian movement and agent-based approaches

The traditional space syntax approach to the study of pedestrian movement in cities, which has been referred to above, could be called ‘aggregative’: it is based on establishing some kind of correlation between an urban indicator, say the integration value of streets in the axial map, and statistical measures of the fluxes of people. Other parameters could be used instead of the integration value of streets—for instance, measures based on the length of the lines of sight, and the extent and shape of the viewshed—but the methodology would still remain the same.

However, a radically different approach to the study of urban movement is possible. Instead of being aggregative, it could be called ‘bottom-up’ or ‘agent based’, and draw on modelling the individual behaviour of pedestrians in a given urban context. These individuals are programmed as agents obeying a number of simple rules; then they are introduced in the urban case-study area under investigation; finally, resulting patterns of movement are observed.

Both methods are acceptable and are not in conflict with each other, as they work best at different scales and tend to highlight different properties of the urban texture. As stated by Batty et al (1998), when discussing agent-based models of pedestrian flow:

“Such approaches, although still novel are not inconsistent with the more aggregative approaches which have dominated urban simulation hitherto, but at scales where buildings, public spaces and streets must be represented as distinct objects, the associated behaviour pattern of individual users must be directly simulated if impacts of changes to the geometry of the local environment are to be understood.”

Agent-based modelling has become topical in recent years, thanks to the significant development of computational resources. The field is now a very active area of research with a vast literature. The aim of this section is not to cover or describe it in detail, but simply to give some hints and show how one agent-based pedestrian model, based on the work by Batty et al (1998), could be implemented on DEMs. The aim is twofold:

(1) to prove the compatibility of the DEM environment with agent-based simulations. This is equivalent to moving map algebra to geo algebra (Couclelis, 1997; Takeyama and Couclelis, 1997). Geo algebra is defined as “a mathematical generalisation of map algebra capable of expressing a variety of dynamic spatial models and spatial data manipulations within a common framework”. Geo algebra includes cellular automata and other agent-based simulations.

(2) And, consequently, to suggest possible ways of integrating agent-based simulations with the techniques for urban analysis described in the previous sections. Information about the lines of sight, the viewshed, etc, could successfully be fed to the agents in order to create more complex behavioural rules.

The algorithm by Batty et al (1998) is partially implemented here. In our case, a binary urban DEM (black and white) defines the walkable parts of the urban environment (streets and squares). Agents are represented by pixels; for visual clarity a colour proportional to the heading has been attributed to each of them, as in figure 26.

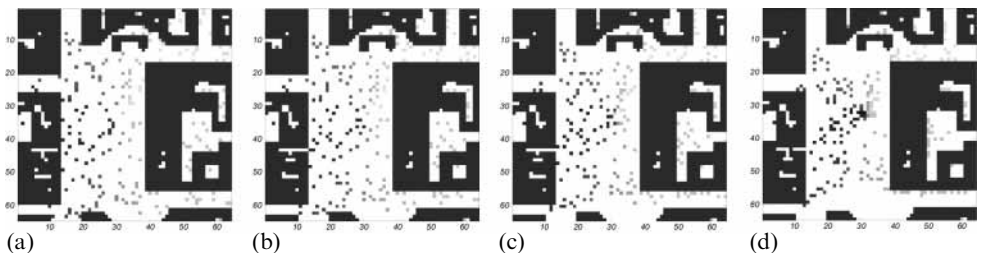


Figure 26. Movement due to the term f_g in Batty et al (1998) after (a) 1, (b) 2, (c) 4, and (d) 8 steps. The colour associated with each agent represents the direction in which it is moving (in radians), based on a standard polar coordinate system centred in the middle of the image.

By developing agent-based pedestrian models on a DEM, a whole range of new possibilities open up. All the knowledge on the urban environment that can be extracted with the algorithms described in the previous sections can be used. Tourist agents (that is, agents who do not have familiarity with the area under investigation) could be programmed to base their choices on the analysis of lines of sight, viewshed, and landmark distribution—as in a kind of navigation based on serendipitous decisionmaking. Conversely, habitués agents, who have familiarity and a better knowledge of the urban environment, might base their movement strategies on finding shortest paths or minimising travelling time between origin and destination. In doing this a differentiation between the behaviour of the different agents would start to appear, as well as multipurpose trips and multicharacteristic profiles. In the algorithm described above, the rules of movement were considered the same for every agent.

Also, during the simulation it would be possible to release urban information to the agents in a gradual way, mimicking a learning process. Information on shortest paths might become available to the agents after they have been walking for a certain amount of time in the street network. This would lead to an infinite number of agent profiles, adaptively varying between zero and full knowledge of the environment (in the latter case, each agent might know the exact position of all other agents and optimise his or her journey accordingly).

At the end of their paper, Batty et al (1998) seem to recognise some limits of commercial software packages when trying to construct agent-based models of pedestrians. They wish “to move to purpose-built software and to relinquish, for a time at least, the powerful graphics and animation capabilities that the current models have.” Matlab and urban DEMs might be the right environment for developing such purpose-built software.

9 Conclusions

The DEM has proven an effective way to store urban geometry and to derive parameters that could complement space syntax. A number of techniques have been presented. Some of them deal with established analyses in the scientific literature, such as lines of sight and viewsheds. Others, such as those related to the accessibility of streets and travelling time, have been introduced, assuming their possible use in deciphering the 'social logic of space'. The list, however, is far from exhaustive: the parameters explored should simply be considered as proofs of the concepts of DEMs. Many additional functions could be defined and coded in Matlab.

No assumption was made on the relationship between urban parameters and, say, pedestrian movement. Traditional space syntax proved this connection by using field surveys and a posteriori correlations between the axial map results and observed movement data (Hillier, 1996). This is beyond the scope of this paper. However, it is worth noting that new techniques are emerging, besides traditional surveys, to describe pedestrian flows. Automatic recognition of human movement from cameras is well advanced, and the development of location-based services attached to most hand-held devices (such as cell-phones, personal digital assistants, or laptops) allows for the first time the real-time monitoring of urban movements. This large data-stream is likely to provide undisputed evidence to validate existing techniques of urban analysis, and probably to suggest new ones.

Also, DEMs are becoming increasingly available. The development of photogrammetry and recent progress in sensing techniques such as laser altimetry and synthetic aperture radar are bound to decrease their cost radically in the coming years. A study of the possible use of DEMs in cities, such as this paper seeks to provide, might therefore be of particular relevance.

Finally, an important aspect of DEM analysis is its downward compatibility with traditional space syntax techniques. Not only tracing of lines of sight, but also the creation of axial maps and the computation of values such as line integration, could be implemented on DEMs. The amount of urban information contained in the DEM is higher than that contained on 2D vectorial supports—and it can easily be reduced to represent the street network as a graph.

References

- Atzwanger K, Schäfer K, 1999, "Evolutionary approaches to the perception of urban spaces" *Evolution and Cognition* 5(1) 87–92
- Batty M, 2001a, "Exploring isovist fields: space and shape in architectural and urban morphology" *Environment and Planning B: Planning and Design* 28 123–150
- Batty M, 2001b, "Visual fields", <http://www.casa.ucl.ac.uk/agent-homepage/visual-fields.htm>
- Batty M, 2004, "A new theory of space syntax", WP 75, Centre for Advanced Spatial Analysis, University College London, <http://www.casa.ucl.ac.uk>
- Batty M, Rana S, 2004, "The automatic definition and generation of axial lines and axial maps" *Environment and Planning B: Planning and Design* 31 615–640
- Batty M, Jiang B, Thurstain-Goodwin M, 1998, "Local movement: agent-based models of pedestrian flow", WP 4, Centre for Advanced Spatial Analysis, University College London, <http://www.casa.ucl.ac.uk>
- Benedikt M L, 1979, "To take hold of space: isovists and isovist fields" *Environment and Planning B: Planning and Design* 6 47–65
- Campos B, 1997, "Strategic space: patterns of use in public squares of the city of London", in *Proceedings of the First International Space Syntax Symposium* (University College London)
- Cormen T H, Leiserson C E, Rivest R L, 1990 *Introduction to Algorithms* (MIT Press, Cambridge, MA)
- Couclelis H, 1997, "From cellular automata to urban models: new principles for model development and implementation" *Environment and Planning B: Planning and Design* 24 165–174
- Douglas D H, 1994, "Least-cost path in GIS using an accumulated cost surface and slopelines" *Cartographica* 31(3) 37–51

-
- Franklin W R, Ray C K, 1994, "Higher isn't necessarily better: visibility algorithms and experiments", in *Advance in GIS Research—Proceedings of the Sixth International Symposium on Spatial Data Handling SDH'96* (University of Edinburgh, Edinburgh) pp 751–770
- Galton F, 1881, "Isochronic passage chart for travellers" *Proceedings of the Royal Geographical Society* **3** 168
- Gibson J J, 1966 *The Senses Considered as Perceptual Systems* (Houghton Mifflin, Boston, MA)
- Hillier B, 1996 *Space is the Machine: A Configurational Theory of Architecture* (Cambridge University Press, Cambridge)
- Hillier B, Penn A, 2004, "Rejoinder to Carlo Ratti" *Environment and Planning B: Planning and Design* **31** 501–511
- Hillier B, Penn A, Hanson J, Grajewski T, Xu J, 1993, "Natural movement: or, configuration and attraction in urban pedestrian movement" *Environment and Planning B: Planning and Design* **20** 29–66
- Lee J, Stucky D, 1998, "On applying viewshed analysis for determining least-cost paths on digital elevation models" *International Journal of Geographical Information Science* **12** 891–905
- Lindgren E S, 1969, "A minimum path problem reconsidered" *Harvard Papers in Theoretical Geography, Geography and the Properties of Surface Series* **28** 1–11
- Llobera M, 2000, "Understanding movement: a pilot model towards the sociology of movement", in *Beyond the Map* Ed. G Lock (IOS Press, Amsterdam) pp 65–84
- Nagy G, 1994, "Terrain visibility" *Computers and Graphics* **18** 763–773
- Oke T R, 1988, "Street design and urban canopy layer climate" *Energy and Buildings* **11** 103–113
- O'Rourke J, 1987 *Art Gallery Theorems and Algorithms* (Oxford University Press, Oxford)
- Peponis J, Wineman J, Rashid M, Bafna S, Kim S H, 1998, "Describing plan configuration according to the covisibility of surfaces" *Environment and Planning B: Planning and Design* **25** 693–708
- Rana S, 2003, "Visibility analysis" *Environment and Planning B: Planning and Design* **30** 641–642
- Ratti C, 2004a, "Space syntax: some inconsistencies" *Environment and Planning B: Planning and Design* **31** 487–499
- Ratti C, 2004b, "Rejoinder to Hillier and Penn" *Environment and Planning B: Planning and Design* **31** 513–516
- Ratti C, Richens P, 2004, "Raster analysis of urban form" *Environment and Planning B: Planning and Design* **31** 297–309
- Steadman P, 2004, "Developments in space syntax" *Environment and Planning B: Planning and Design* **31** 483–486
- Takeyama M, Couclelis H, 1997, "Map dynamics: integrating cellular automata and GIS through geocalgebra" *International Journal of Geographical Information Science* **11**(1) 73–91
- Tomlin C D, 1990 *Geographic Information Systems and Cartographic Modeling* (Prentice-Hall, Englewood Cliffs, NJ)
- Turner A, 2003, "Analysing the visual dynamics of spatial morphology" *Environment and Planning B: Planning and Design* **30** 657–676
- Van Kreveld M, 1996, "Variations on sweep algorithms: efficient computation of extended viewsheds and class intervals", in *Advance in GIS Research II—Proceedings of the Seventh International Symposium on Spatial Data Handling SDH'96* (Delft University of Technology, Delft) II 13A 15–27
- Vasiliev I R, 1997, "Mapping time" *Cartographica* **34**(2) 1–51
- Wang J, Robinson G J, White K, 1996, "A fast solution to local viewshed computation using grid-based digital elevation models" *Photogrammetric Engineering and Remote Sensing* **62** 1157–1164
- Warntz W, 1957, "Transportation, social physics, and the law of refraction" *The Professional Geographer* **9** 2–7

Appendix

Given a number of buildings scattered on a plane, the average length of the lines of sight would be proportional to how regularly they are arranged. In purely random conditions this value is inversely proportional to the size and density of buildings. This fact can be proved with simple mathematics in the simplified case, for instance, of a forest made of tree trunks of uniform diameter. Take a random line of length l . This line intercepts a trunk if the centre of the trunk lies within half a diameter ($d/2$) from the line. Therefore, the average number of trees intercepted by the line can be written (figure A1):

$$N = \rho d.$$

The average length of segments intercepted on the line, measured from trunk centre to trunk centre, is simply

$$S_{\text{from trunk centre}} = \frac{1}{\rho d}.$$

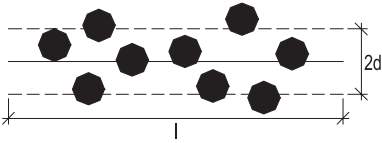


Figure A1. Random distribution of tree trunks in a forest and symbols used in the formula to derive the average length of the lines of sight.

In reality, the interest is not in the distance between trunk centres but between the external parts of the trunks. Therefore a quantity D , $0 < D < d$, should be subtracted. D can be estimated as the average length obtained by randomly cutting a circle of diameter d with lines, which can be proven to be:

$$D = \frac{d}{2}.$$

The average length of the line of sight is therefore:

$$S_{\text{from trunk boundary}} = \frac{1}{\rho d} - \frac{d}{2}.$$

For a density $\rho = 0.01 \text{ m}^{-2}$ (1 trunk every 100 m^2) with a diameter $d = 1 \text{ m}$, the above formula gives:

$$S = \frac{1}{0.01} - 0.5 = 99.5 \text{ m}.$$

If the interest is not in the average values but in the distribution of the length of lines of sight (probability to find a line of sight of $X \text{ m}$), then a similar approach based on the Poisson distribution should be followed.